ORIGINAL RESEARCH

# Assessment of Clinical Stage IA Lung Adenocarcinoma with pN1/N2 Metastasis Using CT Quantitative Texture Analysis

Haixu Zhu[*]
Yanyan Xu[*]
Nanxue Liang
Hongliang Sun [ID]
Zhenguo Huang
Sheng Xie
Wu Wang

[1]Department of Radiology, People's Hospital of Xinjiang Uyghur Autonomous Region, Urumqi 830001, People's Republic of China; [2]Department of Radiology, China–Japan Friendship Hospital, Beijing 100029, People's Republic of China

*These authors contributed equally to this work

**Objective:** To explore the application of texture analysis basing on computed tomography (CT) images in predicting lymph-node metastasis in patients with clinical stage IA lung adenocarcinoma.

**Methods:** In total, 256 patients with clinical stage IA lung adenocarcinoma who had underwentgone preoperative CT examinations were enrolled. A total of 25 texture features using MaZda (version 4.6) software and conventional radiological features were extracted from raw CT data sets. Based on surgical results, patients were stratified into lymph node metastasis–positive and –negative groups. Independent-sample $t$-tests and Mann–Whitney $U$ tests were used to compare continuous variables between the groups. Continuity-correction and $\chi^2$ tests were used for categorical variable comparison. Univariate and multivariate logistic regression analyses were performed to identify independent predictors of lymph-node metastasis.

**Results:** In total, 256 clinical stage IA lung adenocarcinoma cases were proved by pathology: 39 (15.23%) cases with lymph-node metastasis (14 N1a, seven N1b, six N2a1, ten N2a2, and two N2b) and 217 (84.77%) cases without lymph-node metastasis. Univariate and multivariate logistic regression analyses demonstrated that total volume (OR 3.777, $p$=0.015), average CT value of whole tumor (OR 16.271, $p$<0.001), three texture parameters (mean OR 8.473, $p$<0.001; skewness OR 6.393, $p$=0.001; and entropy OR 0.343, $p$=0.049) were independent factors associated with lymph-node status. As such, early-stage lung adenocarcinoma with higher total volume (>4.05 cm$^3$), average CT value of whole tumor (>–70 HU), mean (>133.79), entropy (>1.98), and lower skewness (≤0.02) pointed to positive lymph-node metastasis.

**Conclusion:** Texture parameters were independent factors associated with lymph-node status in clinical stage IA lung adenocarcinoma.

**Keywords:** lung adenocarcinoma, computed tomography, texture, lymph-node metastasis

## Introduction

The introduction of thin-slice computed tomography (TSCT) has greatly improved early detection of small lung adenocarcinomas, with a remarkable reduction in mortality from lung cancer.[1] For clinical stage IA lung adenocarcinoma, ground-glass opacity (GGO) in pulmonary lesions has been reported to be associated with less invasive behavior and good prognosis, and nodules with <50% GGO area demonstrated a great risk of nodal metastasis and poor prognosis.[2,3] Furthermore, according to the International Association for the Study of Lung Cancer–American Thoracic Society–European Respiratory Society classification of lung adenocarcinoma, different

Correspondence: Hongliang Sun
Department of Radiology,
China–Japan Friendship Hospital, Beijing 100029, People's Republic of China
Tel +86 108-420-5514
Fax +86 1064222963
Email stentorsun@gmail.com

pathological subtypes of clinical stage IA lung adenocarcinoma show significant discrepancies in prognosis.[4,5] In addition, the presence of lymph-node metastasis is associated with tumor recurrence and patient survival.[6,7] Treatment regimens, including surgery protocols, have been tailored to early-stage lung cancer with or without lymph-node metastasis.[8]

However, it is quite difficult to exclude tumors' invasive nature and lymph-node metastasis merely based on intraoperative frozen sections in some cases.[4] Previous studies[6,7,9,10] have reported that radiological findings, such as total tumor size, average CT value, ratio of solid areas to whole volume (%solid) on TSCT, and maximum standardized uptake value ($SUV_{max}$) on fluorine-18-fluorodeoxyglucose (FDG) positron-emission tomography (PET)/CT were helpful in predicting the pathological invasiveness of tumors or the prognosis of clinical stage IA lung adenocarcinomas. However, both imaging modalities have demonstrated limited value for identifying malignant involvement of smalllymph nodes in clinical stage IA lung cancer.[6,7]

Currently, texture analysis is an emerging technique that provides objective measurements of heterogeneity based on the distribution of gray levels, and it is not affected by subjective analysis or degree of expertise, inherent limitations of conventional medical imaging interpretation.[11,–12,–31] Promising results of texture analysis have been reported in the field of oncology, especially tumor prognosis, treatment assessment, and differential diagnosis for malignant and benign lymph nodes.[11,–12,–31] However, to our knowledge, there have been few studies investigating its value in predicting lymph-node metastasis in patients with clinical stage IA lung adenocarcinoma.

If some texture parameters derived from preoperative TSCT can predict the risk of nodal involvement before surgery (eg, no metastasis or N1), the mediastinal lymph nodes could be selectively left undissected, especially for patients in poor condition, or neoadjuvant therapy might be prioritized if N2 were discovered before surgery. Therefore, the purpose of this study was to investigate whether texture analysis is useful in predicting lymph-node metastasis in patients with clinical stage IA lung adenocarcinoma, with final surgical sampling as a gold standard.

## Methods
### Patients
Between January 2011 and March 2016, 275 consecutive patients with solitary pulmonary nodules (including subsolid nodules [SSNs]) on CT images underwent surgical resection for adenocarcinoma. Patients were included in this study if they had clinical stage IA lung adenocarcinoma without other lesions in the lung parenchyma, had undergone pulmonary segmentectomy or lobectomy with systematic lymph-node dissection (at least six nodes removed including intrapulmonary, hilar, and mediastinal nodes),[32] and had undergone preoperative TSCT scanning. Exclusion criteria were interval between TSCT examination and surgery >3 months (n=8), neoadjuvant chemotherapy or radiotherapy prior to CT examination (n=5), and history of malignancy in other sites (n=6). The remaining 256 patients — 119 men and 137 women — were enrolled in the current retrospective study. Furthermore, 56 patients had undergone preoperative FDG-PET/CT, which was not routine before operation in our hospital. This retrospective study was approved by the Ethical and Scientific Committees of the China–Japan Friendship Hospital, and informed consent was waived.

### Clinical Characteristics of Patients
Patients' age, sex, smoking status, preoperative serum carcinoembryonic antigen (CEA) level, and tumor sites were obtained and are summarized in Table 1. The cutoff value CEA was set at 5 ng/mL with 95% specificity. as recommended by the manufacturer of the assay kits (Roche Diagnostics, Tokyo, Japan).

### CT Scans and Image Analysis
High-resolution CT scans were performed on either a 16-slice (Toshiba Aquilion) or 320-slice CT scanner (Toshiba Aquilion One). All scans were acquired using a high-resolution volumetric technique. Images were obtained by breath-held helical acquisition in the supine position extending from the lung apices to below the costophrenic angles using parameters of section thickness 5 mm, section intervals 5 mm, pitch 0.75, rotation time 330 ms, tube voltage 120 kV, tube current 200 mA, thin collimation 0.75 mm, and reconstruction matrix 512×512. From raw data, 1 mm–thick section images were reconstructed at 1 mm intervals using a high spatial–frequency algorithm (B60S; Toshiba Aquilion). All CT-scan images were obtained with window settings that were appropriate for lung parenchyma (window width 1,300 Hounsfield units [HU], level −450 HU) and mediastinum (window width 400 HU, level 40 HU). All data were analyzed on the postprocessing workstation EBW4.52 (Extended Brilliant Workshop 4.52, Philips Healthcare Systems).

**Table 1** Textural Parameters Calculated

| | Histogram | Run-length matrix | Gray-level co-occurrence matrix |
|---|---|---|---|
| Level/order | First-order | Second-order | Second-order |
| Description | Histogram where *x*-axis represents pixel/voxel gray level and *y*-axis represents frequency of occurrence | Adjacent or consecutive pixels/voxels of a single gray level in a given direction | How often pairs of pixels with specific values in a specified spatial range occur in an image |
| Parameters | Mean<br>SD<br>Skewness<br>Kurtosis<br>1%<br>10%<br>50%<br>90%<br>99% | Short run–length emphasis<br>Long run–length emphasis<br>Run-length nonuniformity<br>Gray-level nonuniformity<br>Fraction of image in runs | Angular second moment<br>Contrast<br>Correlation<br>Sum of squares<br>Inverse-difference moment<br>Sum average<br>Sum variance<br>Sum entropy<br>Entropy<br>Difference variance<br>Difference entropy |

TSCT features of lung nodules retrospectively evaluated by two radiologists dedicated to thoracic radiology (with 6 and 10 years of experience, respectively) who were blinded to patient clinical data and results from FDG-PET/CT and final surgical sampling were: 1) tumor diameter (TD; cm), defined as maximum axial diameter on lung window; 2) tumor volume (TV; cm$^3$); 3) average CT values of whole tumor (Avg; HU); 3) nodule type — solid (SNs; without GGO in lung window) or SSNs, with GGO in lung window); 4) %solid, defined as the proportion of the solid volume divided by whole TV; 5) air bronchogram (presence or absence); 6) pleural indentation (presence or absence); 7) spiculation (presence or absence); 8) lobulation (presence or absence); and 9) coexistence with bulla or honeycomb (yes or no).

## PET/CT Scans and Image Analysis

FDG-PET/CT scans were available for 56 patients and had been performed within 1 month prior to surgical resection. These studies were all performed on the same PET-CT scanner (Discovery ST; GE Healthcare Life Sciences, Chalfont, UK) using a following protocol of *z*-axis image from the skull base to mid-thigh levels 1 hour after intravenous administration of 7.4 MBq/kg $^{18}$F-FDG (Atom Hi-Tech, Beijing, China). All patients with prescan glucose levels >200 mg/dL fasted for 6 hours prior to the PET/CT scan. Concomitant CT data were used for attenuation correction of PET images and anatomical localization of PET abnormalities. The SUV was adjusted for the injected

dose of $^{18}$F-FDG and the body weight of the patient using the standard software tools provided with the PET-CT scanner.

Another two radiologists with 3 and 6 years of experience in FDG-PET/CT interpretation who were also blinded to patient clinical data and pathological results semiautomatically delineated the outlines of lung lesions, and the activity concentration of $^{18}$F-FDG in the region of interest (ROI) was expressed as SUV. SUV$_{max}$ was defined as the peak SUV of the pixel with the highest counts in the sequential transaxial scans through the ROI, and 2.5 was selected as the cutoff value for a PET/CT-positive result.

## Texture Analysis

Texture analysis was performed on TSCT using dedicated software (MaZda version 4.6, PM Szczypiński, Institute of Electronics, Technical University of Lodz, Poland). For this analysis, ROIs including the whole lesion in TSCT images with the lung window were selected for each subject. In sum, 27 texture parameters, listed in Table 1, were extracted for each ROI on each slice. Run length–matrix parameters were calculated four times for each ROI (vertical, horizontal, 45°, 135°) and gray-level co-occurrence matrix parameters were calculated 20 times for each ROI at a variety of pixel offsets. For comparison of textural features between groups, mean values of run-length and gray-level co-occurrence matrix parameters were used for each ROI, giving a total of 25 parameters to be analyzed
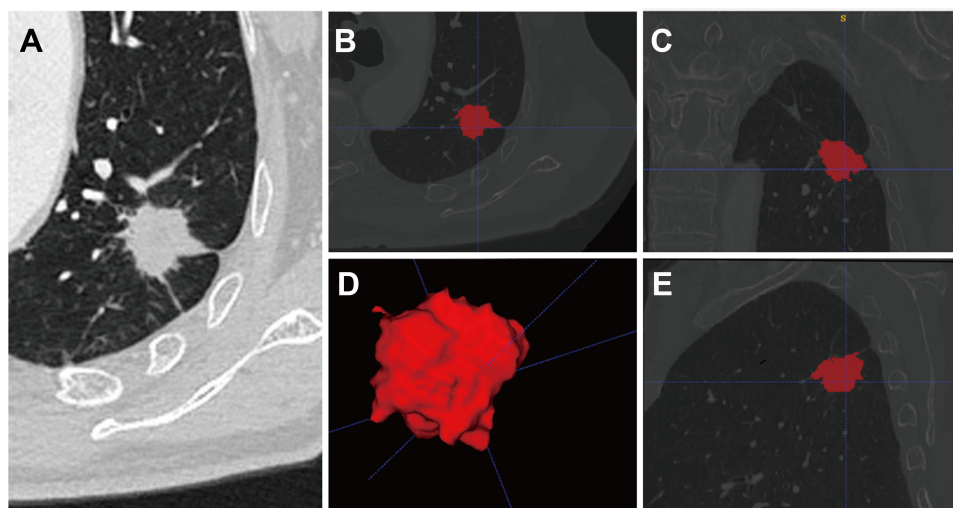
**Figure 1** Lung adenocarcinoma in the apicoposterior segment of the left upper lobe with nodal involvement (N2). (**A**) Axial thin-slice CT image. (**B–E**) Image segmentation and texture processing (**B** axial view, **C** coronal view, **D** volume rendering, **E** sagittal view). TV, Avg, mean, skewness, and entropy values for this lesion were 5.4 cm$^3$, 12 HU, 142.19, −0.02, and 2.03, respectively.
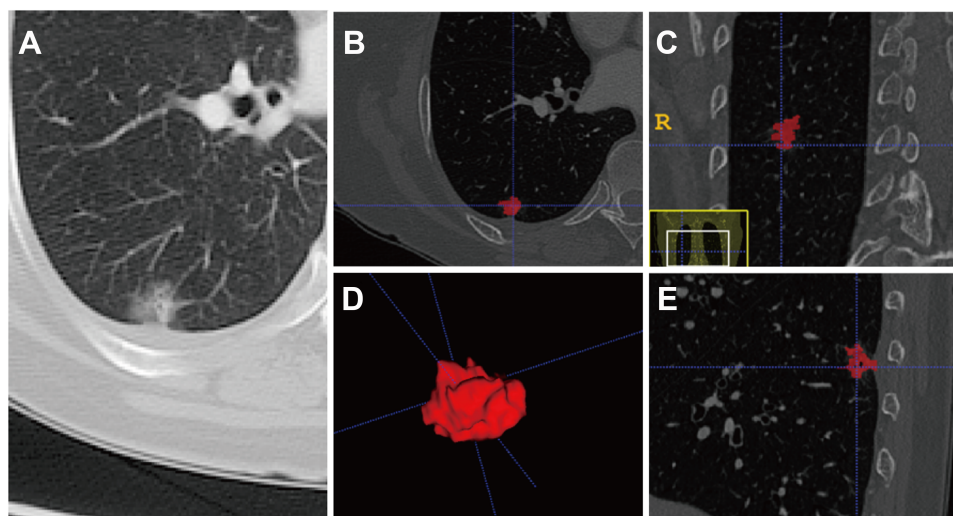


**Figure 2** Images of a lung adenocarcinoma in right lower lobe without nodal involvement. (**A**) Axial thin-slice CT image. (**B–E**) Image segmentation and texture processing (**B** axial view, **C** coronal view, **D** volume rendering, **E** sagittal view). The TV, Avg, Mean, Skewness and Entropy values for this lesion were 1.8 cm$^3$, −110 Hu, 84.53, 1.39 and 1.67, respectively.

(Figures 1 and 2). A more detailed description of the texture parameters calculated has been reported in previous studies.[33,34]

## Pathology Analysis

Hematoxylin–eosin staining of tissue slices and pathological evaluation were performed for all 256 pulmonary specimens by two pathologists (with 8 and 19 years of experience, respectively) according to the eighth edition of the *TNMClassification of Malignant Tumours*.[35,36] The final results revealed 39 patients with positive lymph-node metastasis (including 21 N1 and 18 N2) and 217 with negative lymph-node metastasis.

## Statistical Analysis

All data were evaluated using SPSS17.0 (SPSS, Chicago, IL, USA). Descriptive statistics are provided as means ± SD or medians ± IQR for continuous variables and as frequency and percentage for categorical variables. According to surgical results, patients were stratified into lymph node metastasis–positive and –negative groups. Independent-sample *t*-tests and Mann–Whitney *U* tests were used to compare

continuous variables between the groups. The $\chi^2$ and continuity-correction tests were used for categorical-variable comparison between the groups. Univariate and multivariate logistic regression analyses were performed to identify independent predictors for lymph-node metastasis. $P<0.05$ was considered statistically significant.

## Results

In total, there were 256 pathologically proven clinical stage IA lung adenocarcinoma cases: 153 (59.77%) SNs and 103 (40.23%) SSNs. A total of 39 (15.23%) cases had lymph-node metastasis (fourteen N1a, seven N1b, six N2a1, ten N2a2, and two N2b) and 217 (84.77%) did not. Conventional radiological findings and basic clinical information are summarized in Table 2.

## Univariate Analysis

Conventional radiological findings and clinical characteristics of patients with different lymph-node status are shown in Table 3. For the lymph node–metastasis group, larger TD and TV and higher Avg and preoperative serum

CEA were observed ($p<0.001$, $p=0.018$, $p=0.005$, and $p<0.001$, respectively). With regard to conventional high-resolution CT features, the presence of SNs and coexistence with bulla/honeycomb were more frequently observed in the metastasis-positive group than the metastasis-negative group (both $p=0.001$). For clinical stage IA lung adenocarcinoma, mean values of 13 of 25 textural parameters were significantly different in patients with different lymph-node status. The results of textural features are summarized in Table 4.

## Multivariate Analysis

TD, TV, Avg, preoperative serum CEA, nodule type, coexistence with bulla/honeycomb, and 13 of 25 textural parameters were subjected to binary logistic regression analysis. TD was analyzed as a continuous variable. The results demonstrated that TV (OR 3.777, 95% CI 1.298–10.989; $p=0.015$), Avg (OR 16.271, 95% CI 5.130–51.609; $p<0.001$), mean (OR 8.473, 95% CI 2.706–26.529; $p<0.001$), skewness (OR 6.393, 95% CI 2.193–18.634; $p=0.001$), and entropy (OR 0.343, 95% CI 0.118–0.994;

**Table 2** Summary of Radiological Features and Patients' Clinical Characteristics (n=256)

| | n/value | Factors | n/value |
|---|---|---|---|
| **Age (years)** | 62.3±10.4 | SN | 153 (59.77%) |
| **Sex** | | SSN | 103 (40.23%) |
| Male | 119 (46.48%) | %solid | |
| Female | 137 (53.52%) | ≥50% | 218 (85.16%) |
| **Smoking status** | | <50% | 38 (14.84%) |
| Smoker | 79 (30.86%) | Air bronchogram | |
| Nonsmoker | 177 (69.14%) | Yes | 91 (35.55%) |
| **Preoperative serum CEA** | | No | 165 (64.45%) |
| ≥5 ng/mL | 60 (23.44%) | Pleural indentation | |
| <5 ng/mL | 196 (76.56%) | Yes | 162 (63.28%) |
| **SUV$_{max}$*** | | No | 94 (36.72%) |
| ≥2.5 | 38 (67.86%) | Spiculation | |
| <2.5 | 18 (32.14%) | Yes | 89 (34.77%) |
| **Tumor site** | | No | 167 (65.23%) |
| RUL/RML/RLL | 80/13/55 | Lobulation | |
| LUL/LLL | 60/48 | Yes | 200 (78.13%) |
| **TD (cm)** | 2.11±0.68 | No | 56 (21.87%) |
| **TV (cm$^3$)$^\Delta$** | 2.30±2.87 | Coexistence with bulla or honeycomb | |
| **Avg (HU)$^\Delta$** | −105.50±128.25 | Yes | 51 (19.92%) |
| **Nodule type** | | No | 205 (80.08%) |

**Notes**: Continuous variables expressed as means ± SD or medians ± IQR. $^\Delta$Medians ± IQR. *The results of FDG-PET/CT scan were only available in 56 patients, since they did not have medical insurance.
**Abbreviations**: CEA, carcinoembryonic antigen; SUV$_{max}$, maximum standardized uptake value; RUL, right upper lobe; RML, right middle lobe; RLL, right lower lobe; LUL, left upper lobe; LLL, left lower lobe; TD, tumor diameter; TV, tumor volume; Avg, average CT values of whole tumor; SN, solid nodule; SSN, subsolid nodule.

**Table 3** Conventional Radiological Findings and Clinical Characteristics of Patients with Different Lymph-Node Status

| | Lymph-Node Status | | p |
|---|---|---|---|
| | Metastasis-Positive (n=39) | Metastasis-Negative (n=217) | |
| **Age (years)*** | 61.13±8.72 | 62.38±10.36 | 0.477 |
| **Sex (male/female)** | | | 0.317 |
| Male | 21 (8.20%) | 98 (38.28%) | |
| Female | 18 (7.03%) | 119 (46.48%) | |
| **Smoking status** | | | 0.989 |
| Smoker | 12 (4.69%) | 67 (26.17%) | |
| Nonsmoker | 27 (10.55%) | 150 (58.59%) | |
| **Preoperative serum CEA** | | | <0.001 |
| ≥5 ng/mL | 20 (7.81%) | 40 (15.63%) | |
| <5 ng/mL | 19 (7.42%) | 177 (69.14%) | |
| **$SUV_{max}$** | | | 0.692 |
| ≥2.5 | 5 (8.93%) | 33 (58.93%) | |
| <2.5 | 1 (0.11%) | 17 (30.36%) | |
| **Tumor site** | | | 0.586 |
| Right lung | 21 (8.20%) | 127 (49.61%) | |
| Left lung | 18 (7.03%) | 90 (35.16%) | |
| **TD (cm)** | 2.51±0.70 | 2.04±0.65 | <0.001 |
| **TV (cm³)△** | 5.40±5.80 | 2.10±2.30 | <0.001 |
| **Avg (HU)△** | −20.00±68.00 | −114.00±136.00 | <0.001 |
| **%solid** | | | 0.699 |
| ≥50% | 34 (13.28%) | 184 (71.88%) | |
| <50% | 5 (1.95%) | 33 (12.89%) | |
| **Nodule type** | | | 0.001 |
| SN | 33 (12.89%) | 120 (46.88%) | |
| SSN | 6 (2.34%) | 97 (37.89%) | |
| **Air bronchogram** | | | 0.298 |
| Yes | 11 (4.30%) | 80 (31.25%) | |
| No | 28 (10.94%) | 137 (53.51%) | |
| **Pleural indentation** | | | 0.119 |
| Yes | 29 (11.33%) | 133 (51.95%) | |
| No | 10 (3.91%) | 84 (32.81%) | |
| **Spiculation** | | | 0.105 |
| Yes | 18 (7.03%) | 71 (27.73%) | |
| No | 21 (8.20%) | 146 (57.03%) | |
| **Lobulation** | | | 0.823 |
| Yes | 31 (12.11%) | 169 (66.02%) | |
| No | 8 (3.12%) | 48 (18.75%) | |

(*Continued*)

**Table 3** (Continued).

| | Lymph-Node Status | | p |
|---|---|---|---|
| | Metastasis-Positive (n=39) | Metastasis-Negative (n=217) | |
| **Coexistence with bulla/honeycomb** | | | <0.001 |
| Yes | 20 (7.81%) | 31 (12.11%) | |
| No | 19 (7.42%) | 186 (72.66%) | |

**Notes**: Continuous variables in the table expressed as means ± SD or medians ± IQR. *Means ± SD; △medians ± IQR.

p=0.049) were independent factors associated with lymph-node status in clinical stage IA lung adenocarcinoma (Table 5). Detailed information regarding receiver operating characteristic (ROC) analysis for the aforementioned five parameters is described in Supplementary Table 1. Early lung adenocarcinoma with higher TV (>4.05 cm³), Avg (>−70 HU), mean (>133.79), and entropy (>1.98) and lower skewness (≤0.02) tended to demonstrate positive lymph-node metastasis.

## Discussion

In the present investigation, we found that TV, Avg, and high-resolution CT images based on texture features (mean, skewness, entropy) were associated with lymph-node status in clinical stage I adenocarcinoma. In addition to conventional features, texture features related to heterogeneity in lesions were also able to be further extracted from high-resolution CT images to provide complementary information for predicting lymph-node metastasis. Our preliminary results provided evidence for the potential application of texture analysis in lung cancer.

It has been well proven that heterogeneity is a vital feature of malignancy. Various alternations in tissue architecture resulting from cell infiltration, necrosis, abnormal angiogenesis, and myxoid changes lead to heterogeneity,[15,37,38] which is associated with adverse tumor biology.[15,–23,–24,–39–41] A previous study suggested that CT heterogeneity measured by texture analysis may reflect vascularization in tissue,[42] and Ganeshan et al further confirmed the correlation between CT-texture parameters and histopathological features of hypoxia and angiogenesis in non–small cell lung cancer.[13] In addition, tumor heterogeneity evaluated by CT has yielded promising results in various cancers for diagnosis, staging/prognostication, and treatment-response assessment.[12,13,16–18,21,25–27] As far as

**Table 4** Texture-Analysis Results in Patients with Different Lymph-Node Status

| | Lymph-Node Status | | p |
|---|---|---|---|
| | Metastasis-Positive | Metastasis-Negative | |
| **Histogram** | | | |
| Mean | 150.99±33.77 | 120.63±37.66 | <0.001 |
| SD | 2,177.77±1,118.29 | 1,698.62±961.81 | 0.006 |
| Skewness | −0.06±1.17 | 0.30±0.80 | 0.001 |
| Kurtosis | −0.66±0.80 | −0.55±0.88 | 0.491 |
| 1% | 55.00±43.00 | 46.00±24.00 | 0.046 |
| 10% | 81.00±51.00 | 65.00±35.00 | 0.003 |
| 50% | 151.82±42.19 | 118.16±43.20 | <0.001 |
| 90% | 212.00±29.00 | 181.00±76.00 | <0.001 |
| 99% | 234.00±23.00 | 217.00±52.50 | <0.001 |
| **Run-length matrix** | | | |
| Short run–length emphasis | 0.98±0.01 | 0.99±0.01 | 0.209 |
| Long run–length emphasis | 1.03±0.02 | 1.03±0.03 | 0.211 |
| Run-length nonuniformity | 134.76±63.28 | 107.77±60.37 | 0.003 |
| Gray-level nonuniformity | 2.30±0.81 | 2.14±0.74 | 0.211 |
| Fraction of image in runs | 0.99±0.01 | 0.98±0.02 | 0.368 |
| **Gray-level co-occurrence matrix** | | | |
| Angular second moment ($\times10^3$) | 14.64±6.24 | 18.54±10.27 | 0.022 |
| Contrast | 971.52±364.76 | 930.47±442.55 | 0.585 |
| Correlation | 0.70±0.11 | 0.71±0.13 | 0.849 |
| Sum of squares | 1,683.95±116.65 | 1,680.75±157.82 | 0.904 |
| Inverse-difference moment ($\times10^3$) | 62.58±29.41 | 62.70±36.96 | 0.984 |
| Sum average | 252.93±8.17 | 254.54±7.73 | 0.235 |
| Sum variance | 5,764.73±607.73 | 5,791.37±741.91 | 0.832 |
| Sum entropy | 1.58±0.15 | 1.49±0.18 | 0.007 |
| Entropy | 1.92±0.17 | 1.83±0.19 | 0.005 |
| Difference variance | 394.53±168.47 | 357.32±160.08 | 0.186 |
| Difference entropy | 1.39±0.13 | 1.33±0.18 | 0.001 |

**Notes**: Continuous variables expressed as means ± SD or medians ±IQR.

we know, there have been few studies that have quantitatively assessed tumor heterogeneity using texture analysis to predict lymph-node metastasis in early-stage adenocarcinoma.[43]

In our current study, entropy was associated with lymph-node metastasis (OR 0.343, 95% CI 0.118–0.994; p=0.049). Entropy represents texture irregularity in tissue, and higher entropy means increased heterogeneity of the tissue.[27,28] Furthermore, higher entropy was also associated with higher tumor stage. Therefore, it is plausible that higher entropy (>1.98) was related to positive lymph-node metastasis in the current study. In addition, tumors with higher mean (>133.79) and lower skewness (≤0.02) were also prone to positive lymph-node metastasis. Our results align with those reported in previous studies;[12,14,29,30] however, it is challenging to compare

detailed texture features due to variable factors, such as the choice of disease, tumor stage, various modalities of raw images, and commercial software vendor. Future work needs to be done to generate a widely applicable, uniform standard for texture-analysis methodology.

In addition, it has been reported that volumetric analysis of pulmonary lesions on a three-dimensional scale would be more objective and accurate,[9,19–22] and Avg (OR 32.210, 95% CI 3.020–79.689; p<0.001) is correlated with pathological risk classification in clinical stage IA lung adenocarcinoma. In our study, a similar trend was observed. The volumetric result of Avg was a significant independent predictor of lymph-node metastasis. Interestingly, although GGO area <50% was considered a predictor for poor prognosis,[2,3] %solid set to the same cutoff point (50%) demonstrated no

**Table 5** Independent Factors Associated with Lymph-Node Metastasis

|  | OR (95% CI) | p |
|---|---|---|
| Avg | 16.271 (5.130–51.609) | <0.001 |
| Mean | 8.473 (2.706–26.529) | <0.001 |
| Skewness | 6.393 (2.193–18.634) | 0.001 |
| TV | 3.777 (1.298–10.989) | 0.015 |
| Entropy | 0.343 (0.118–0.994) | 0.049 |
| Preoperative serum CEA | NA | 0.523 |
| TD | NA | 0.349 |
| Nodule type | NA | 0.761 |
| Coexistence with bulla/ honeycomb | NA | 0.271 |
| SD | NA | 0.929 |
| 1% | NA | 0.576 |
| 10% | NA | 0.605 |
| 50% | NA | 0.126 |
| 90% | NA | 0.541 |
| 99% | NA | 0.831 |
| Run-length nonuniformity | NA | 0.620 |
| Angular second moment | NA | 0.818 |
| Sum entropy | NA | 0.698 |
| Difference entropy | NA | 0.739 |

**Note**: Binary logistic regression analysis with forward conditional method.
**Abbreviations**: Avg, average CT values of whole tumor; TV, tumor volume; CEA, carcinoembryonic antigen; TD, tumor diameter; NA, not associated.

significant differences between different lymph-node status. One possible reason was that limited SSNs were enrolled in our study. Moreover, the measuring methods were different for GGO ratio and %solid. The former was evaluated by two-dimensional, semi-quantitative measurement, while the value of %solid was decided by volumetric, quantitative measurement.[10] Further investigation with more SSN samples enrolled needs to be done to verify our results.

Our results demonstrated that quantitative texture analysis and volumetric measurement of lung lesions had the potential to predict lymph-node metastasis in patients with clinical stage IA stage adenocarcinoma. Texture analysis can be performed on routinely existing data (eg, CT)[12,13,16–18,21,25–27] without additional ionizing radiation or significant extra cost, and provide encouragingly supplementary information, especially for patients with lymph nodes too small to be characterized on FDG-PET/CT or inconclusive endobronchial ultrasound–sampling results.

Although encouraging, this study has several limitations. First, a relatively small sample was included. Given the small sample, we limited our focus to three categories

of texture features for predicting lymph-node metastasis. Second, the study was retrospective in nature and selection bias was present. Only patients with systematic lymph-node dissection were enrolled in the final analysis. Third, lymph-node status was divided only into metastasis-positive and -negative groups. Also, potential differences in radiological findings between patients with N1 and N2 metastasis were not described in the current study, due to a small cohort of patients. Fourth, all the results were derived from a single institution using the same texture-analysis software. Fifth, two CT scanners (16-slice and 320-slice CT) were used. However, the two scanners were provided by the same vendor and scan parameters were carefully adjusted to the same conditions. What is more, it has been reported that CT-texture features extracted from first-order statistics are fairly reproducible.[31] Therefore, there is little reason to suspect the robustness of CT-texture features in our current study.

## Conclusion

In conclusion, our results demonstrated that texture parameters (mean, skewness, and entropy) were independent factors associated with lymph-node status in clinical stage IA lung adenocarcinoma. In other words, quantitative CT-texture analysis showed potential value in predicting nodal involvement in patients with early-stage lung adenocarcinoma, which may assist in surgical decision-making to some degree.

## Abbreviations

TSCT, thin-slice computed tomography; TD, tumor diameter; SN, solid nodule; SSN, subsolid nodule; TV, tumor volume; Avg, average CT values of whole tumor; GGO, ground-glass opacity; SUV, standardized uptake value; FDG-PET/CT, fluorine-18-fluorodeoxyglucose positron–emission tomography/computed tomography; CEA, carcinoembryonic antigen; HU, Hounsfield units; ROI, region of interest; NSCLC, non–small cell lung cancer; ROC, receiver-operating characteristic.

## Data-Sharing Statement

Please contact the corresponding author for data requests.

## Ethics Approval and Consent to Participate

This retrospective study was approved by our institutional ethics committee (IRB code: 2017–17). It was determined

to be a retrospective analysis of deidentified data andexempt from requiring written informed consent.

## Author Contributions

All authors contributed to data analysis, drafting or revising the article, gave final approval to the version to be published, and agree to be accountable for all aspects of the work.

## Funding

## Disclosure

The authors report no conflicts of interest in this work.

## References

1. Aberle DR, Adams AM, Berg CD, et al. Reduced lung-cancer mortality with low-dose computed tomographic screening. *N Engl J Med*. 2011;365:395–409.
2. Kodama K, Higashiyama M, Yokouchi H, et al. Prognostic value of ground-glass opacity found in small lung adenocarcinoma on high-resolution CT scanning. *Lung Cancer*. 2001;33:17–25. doi:10.1016/S0169-5002(01)00185-4
3. Asamura H, Hishida T, Suzuki K, et al. Radiographically determined noninvasive adenocarcinoma of the lung: survival outcomes of Japan Clinical Oncology Group 0201. *J Thorac Cardiovasc Surg*. 2013;146 (1):24–30. doi:10.1016/j.jtcvs.2012.12.047
4. Yoshizawa A, Motoi N, Riely GJ, et al. Impact of proposed IASLC/ATS/ERS classification of lung adenocarcinoma: prognostic subgroups and implications for further revision of staging based on analysis of 514 stage I cases. *Mod Pathol*. 2011;24(5):653–664. doi:10.1038/modpathol.2010.232
5. Travis WD, Brambilla E, Noguchi M, et al. International Association for the Study of Lung Cancer/American Thoracic Society/European Respiratory Society: international multidisciplinary classification of lung adenocarcinoma: executive summary. *Proc Am Thorac Soc*. 2011;8(5):381–385. doi:10.1513/pats.201107-042ST
6. Darling GE, Maziak DE, Inculet RI. Positron emission tomography-computed tomography compared with invasive mediastinal staging in non-small cell lung cancer: results of mediastinal staging in the early lung positron emission tomography trial. *J Thorac Oncol*. 2011;6(8):1367–1372. doi:10.1097/JTO.0b013e318220c912
7. Harders SW, Madsen HH, Hjorthaug K. Mediastinal staging in non-small-cell lung carcinoma: computed tomography versus F-18-fluorodeoxyglucose positron-emission tomography and computed tomography. *Cancer Imaging*. 2014;14(1):23. doi:10.1186/1470-7330-14-23
8. Darling GE, Allen MS, Decker PA, et al. Randomized trial of mediastinal lymph node sampling versus complete lymphadenectomy during pulmonary resection in the patient with N0 or N1 (less than hilar) non-small cell carcinoma: results of the American College of Surgery Oncology Group Z0030 Trial. *J Thorac Cardiovasc Surg*. 2011;141:662–670. doi:10.1016/j.jtcvs.2010.11.008

9. Lv Y-L, Yuan D-M, Wang K. Diagnostic performance of integrated positron emission tomography/computed tomography for mediastinal lymph node staging in non-small cell lung cancer: a bivariate systematic review and meta-analysis. *J Thorac Oncol*. 2011;6(8):1350–1358. doi:10.1097/JTO.0b013e31821d4384
10. Li Z, Ye B, Bao M, et al. Radiologic predictors for clinical stage IA lung adenocarcinoma with ground glass components: a multi-center study of long-term outcomes. *PLoS One*. 2015;10(9):e0136616. doi:10.1371/journal.pone.0136616
11. Kassner A, Thornhill RE. Texture analysis: a review of neurologic MR imaging applications. *AJNR Am J Neuroradiol*. 2010;31 (5):809–816. doi:10.3174/ajnr.A2061
12. Bayanati H, Thornhill RE, Souza CA, et al. Quantitative CT texture and shape analysis: can it differentiate benign and malignant mediastinal lymph nodes in patients with primary lung cancer? *Eur Radiol*. 2015;25(2):480–487. doi:10.1007/s00330-014-3420-6
13. Ganeshan B, Goh V, Mandeville HC, Ng QS, Hoskin PJ, Miles KA. Non-small cell lung cancer: histopathologic correlates for texture parameters at CT. *Radiology*. 2013;266(1):326–336. doi:10.1148/radiol.12112428
14. Ganeshan B, Abaleke S, Young RC, Chatwin CR, Miles KA. Texture analysis of non-small cell lung cancer on unenhanced computed tomography: initial evidence for a relationship with tumour glucose metabolism and stage. *Cancer Imaging*. 2010;10:137–143. doi:10.1102/1470-7330.2010.0021
15. Ganeshan B, Panayiotou E, Burnand K, Dizdarevic S, Miles K. Tumour heterogeneity in non-small cell lung carcinoma assessed by CT texture analysis: a potential marker of survival. *Eur Radiol*. 2012;22(4):796–802. doi:10.1007/s00330-011-2319-8
16. Ahn SY, Park CM, Park SJ, et al. Prognostic value of computed tomography texture features in non-small cell lung cancers treated with definitive concomitant chemoradiotherapy. *Invest Radiol*. 2015;50(10):719–725. doi:10.1097/RLI.0000000000000174
17. Wu J, Aguilera T, Shultz D, et al. Early-stage non-small cell lung cancer: quantitative imaging characteristics of (18)F fluorodeoxyglucose PET/CT allow prediction of distant metastasis. *Radiology*. 2016;281(1):270–278. doi:10.1148/radiol.2016151829
18. Fried DV, Tucker SL, Zhou S, et al. Prognostic value and reproducibility of pretreatment CT texture features in stage III non-small cell lung cancer. *Int J Radiat Oncol Biol Phys*. 2014;90(4):834–842. doi:10.1016/j.ijrobp.2014.07.020
19. Ravanelli M, Farina D, Morassi M, et al. Texture analysis of advanced non-small cell lung cancer (NSCLC) on contrast-enhanced computed tomography: prediction of the response to the first-line chemotherapy. *Eur Radiol*. 2013;23(12):3450–3455. doi:10.1007/s00330-013-2965-0
20. Dennie C, Thornhill R, Souza CA, et al. Quantitative texture analysis on pre-treatment computed tomography predicts local recurrence in stage I non-small cell lung cancer following stereotactic radiation therapy. *Quant Imaging Med Surg*. 2017;7(6):614–622. doi:10.21037/qims.2017.11.01
21. Andersen MB, Harders SW, Ganeshan B, Thygesen J, Torp Madsen HH, Rasmussen F. CT texture analysis can help differentiate between malignant and benign lymph nodes in the mediastinum in patients suspected for lung cancer. *Acta Radiol*. 2016;57(6):669–676. doi:10.1177/0284185115598808
22. Al-Kadi OS, Watson D. Texture analysis of aggressive and nonaggressive lung tumor CE CT images. *IEEE Trans Biomed Eng*. 2008;55:1822–1830. doi:10.1109/TBME.2008.919735
23. Win T, Miles KA, Janes SM, et al. Tumor heterogeneity and permeability as measured on the ct component of pet/ct predict survival in patients with non-small cell lung cancer. *Clin Cancer Res*. 2013;19 (13):3591–3599. doi:10.1158/1078-0432.CCR-12-1307

24. Cook GJ, Yip C, Siddique M, et al. Are pretreatment 18f-fdg pet tumor textural features in non-small cell lung cancer associated with response and survival after chemoradiotherapy? *J Nucl Med*. 2013;54 (1):19–26. doi:10.2967/jnumed.112.107375

25. Gevaert O, Xu J, Hoang CD, et al. Non-small cell lung cancer: identifying prognostic imaging biomarkers by leveraging public gene expression microarray data–methods and preliminary results. *Radiology*. 2012;264:387–396. doi:10.1148/radiol.12111607

26. Mattonen SA, Palma DA, Haasbeek CJA, et al. Distinguishing radiation fibrosis from tumour recurrence after stereotactic ablative radiotherapy (SABR) for lung cancer: a quantitative analysis of ct density changes. *Acta Oncol*. 2013;52(5):910–918. doi:10.3109/028418 6X.2012.731525

27. Son JY, Lee HY, Lee KS, et al. Quantitative CT analysis of pulmonary ground-glass opacity nodules for the distinction of invasive adenocarcinoma from pre-invasive or minimally invasive adenocarcinoma. *PLoS One*. 2014;9(8):e104066. doi:10.1371/journal.pone.0104066

28. Kim J-H, Ko ES, Lim Y, et al. Breast cancer heterogeneity: MR imaging texture analysis and survival outcomes. *Radiology*. 2016;160261.

29. Kim SY, Lee E, Nam SJ, et al. Ultrasound texture analysis: association with lymph node metastasis of papillary thyroid microcarcinoma. *PLoS One*. 2017;12(4):e0176103. doi:10.1371/journal.pone.0176103

30. Ng F, Ganeshan B, Kozarski R, Miles KA, Goh V. Assessment of primary colorectal cancer heterogeneity by using whole-tumor texture analysis: contrast-enhanced CT texture as a biomarker of 5-year survival. *Radiology*. 2013;266(1):177–184. doi:10.1148/radiol.12120254

31. Lubner MG, Smith AD, Sandrasegaran K, et al. CT texture analysis: definitions, applications, biologic correlates, and challenges. *Radiographics*. 2017;37(5):1483-1503. doi:10.1148/rg.2017170056

32. Lardinois D, De Leyn P, Van Schil P, et al. ESTS guidelines for intraoperative lymph node staging in non-small cell lung cancer. *Eur J Cardiothorac Surg*. 2006;30(5):787–792. doi:10.1016/j.ejcts.20 06.08.008

33. Haralick R, Shanmugam K, Dinstein I. Textural features for image classification. *IEEE Trans Syst Man Cybern*. 1973;SMC-3 (6):610–621. doi:10.1109/TSMC.1973.4309314

34. Schieda N, Thornhill RE, Al-Subhi M, et al. Diagnosis of sarcomatoid renal cell carcinoma with CT: evaluation by qualitative imaging features and texture analysis. *AJR Am J Roentgenol*. 2015;204 (5):1013–1023. doi:10.2214/AJR.14.13279

35. Brierley JD, Gospodarowicz MK, Wittekind C, eds. *UICC TNM Classification of Malignant Tumours*. 8th ed. Oxford: Wiley Blackwell; 2017.

36. Rami-Porta R, Call S, Dooms C, et al. Lung cancer staging: a concise update. *Eur Respir J*. 2018;51(5):1800190. doi:10.1183/139930 03.00190-2018

37. Lunt SJ, Chaudary N, Hill RP. The tumor microenvironment and metastatic disease. *Clin Exp Metastasis*. 2009;26(1):19–34. doi:10.1007/s10585-008-9182-2

38. Davnall F, Yip CSP, Ljungqvist G, et al. Assessment of tumor heterogeneity: an emerging imaging tool for clinical practice? *Insights Imaging*. 2012;3(6):573–589. doi:10.1007/s13244-012-0196-6

39. Tixier F, Le Rest CC, Hatt M, et al. Intratumor heterogeneity characterized by textural features on baseline 18F-FDG PET images predicts response to concomitant radiochemotherapy in esophageal cancer. *J Nucl Med*. 2011;52(3):369–378. doi:10.2967/jnumed.11 0.082404

40. Cook GJ, O'Brien ME, Siddique M, et al. Non-small cell lung cancer treated with erlotinib: heterogeneity of (18)F-FDG uptake at PET-association with treatment response and prognosis. *Radiology*. 2015;276(3):883–893. doi:10.1148/radiol.2015141309

41. Tixier F, Hatt M, Valla C, et al. Visual versus quantitative assessment of intratumor 18F-FDG PET uptake heterogeneity: prognostic value in non-small cell lung cancer. *J Nucl Med*. 2014;55(8):1235–1241. doi:10.2967/jnumed.113.133389

42. Bézy-Wendling J, Kretowski M, Rolland Y, Le Bidon W. Toward a better understanding of texture in vascular CT scan simulated images. *IEEE Trans Biomed Eng*. 2001;48(1):120–124. doi:10.1109/10.900272

43. Liu Y, Kim J, Balagurunathan Y, et al. Prediction of pathological nodal involvement by CT-based radiomic features of the primary tumor in patients with clinically node-negative peripheral lung adenocarcinomas. *Med Phys*. 2018;45(6):2518–2526. doi:10.1002/mp.12901